# Supplement

**Model structure.** Six major compartments in the model depicted in Figures 2a and 2b (main text) reflect the natural history of tuberculosis and host HIV status (a superscript '+' in all notation below indicates a state or a parameter that corresponds to a host with HIV infection):

- $S$ and $S^+$ – Susceptible to infection by *M. tuberculosis*;
- $L$ and $L^+$ – Latently infected with *M. tuberculosis*;
- $I$ and $I^+$ – Active disease with *M. tuberculosis*.

Several of these compartments are further subdivided to reflect: 1) additional details about the drug-resistance and fitness of the *M. tuberculosis* strain with which individuals may be infected and 2) risk of infection with HIV. First, for those with latent infection or disease with TB, we classify all the TB strains according to their number of anti-TB drugs to which the strain is resistant ($n$) and number of compensation events ($k \le n$):

$$\begin{aligned} L &\equiv \sum_{n,k} L_{n,k} \\ L^+ &\equiv \sum_{n,k} L^+_{n,k} \\ I &\equiv \sum_{n,k} I_{n,k} \\ I^+ &\equiv \sum_{n,k} I^+_{n,k} \end{aligned} . \qquad \text{(S1)}$$

The mycobacterial state $(n,k)$ may change as a result of two events: 1) inadequate treatment may result in selection of mycobacteria with additional resistance which leads to an increase in $n$ and a subsequent reduction in fitness in the absence of drug treatment; or 2) sporadic mutation may occur that compensates for a fraction of the fitness cost associated with resistance which leads to an increase in $k$:

$$\begin{aligned} (n,k) &\to (n+1,k) \qquad \textit{acquisition of DR} \\ (n,k) &\to (n,k+1) \qquad \textit{compensation};\ k < n \end{aligned} . \qquad \text{(S2)}$$

Second, we assume that only a fraction of the population is at risk of HIV infection. This is modeled by placing a fixed proportion of individuals born into the model into a part of the model where they do not experience an HIV force of infection. This approach is used in other simple models of HIV [71] and allows for the model to fit observed data for both the timing of rapid emergence of HIV and levels of endemic HIV prevalence. The cost of this assumption is that the fractions of HIV-susceptible among TB-susceptibles ($v_S \in (0,1)$) and latently infected ($v_{n,k} \in (0,1)$) have to be considered as variables, increasing the total number of differential equations. For simplicity, we do not allow the individuals with active TB to be infected by HIV; this has minimal effects as TB disease is rare and thus the relative size of this compartment is very small.

The full set of dynamic equations is presented below and Table S1 provides the full list of the parameters with descriptions and ranges used in the sensitivity/uncertainty analyses.

$$
\begin{aligned}
&\tfrac{d}{dt}S = \mu - \left(\mu + \sum_{n,k}\lambda_{n,k} + v_S\lambda^h\right)S \\
&\tfrac{d}{dt}v_S = \left(z - v_S\right)\mu/S - v_S\left(1 - v_S\right)\lambda^h \\
&\tfrac{d}{dt}S^+ = v_S\lambda^h S - \left(\mu^+ + \sum_{n,k}\lambda_{n,k}\right)S^+ \\
&\tfrac{d}{dt}L_{n,k} = \left(1 - p_{n,k}\right)\lambda_{n,k}S + \left(h + \left(1 - q_n\right)\gamma\right)I_{n,k} - \left(\mu + \pi_{n,k} + v_{n,k}\lambda^h + \varepsilon\sum_{n,k}p_{n,k}\lambda_{n,k}\right)L_{n,k} \\
&\tfrac{d}{dt}v_{n,k} = \left(1 - p_{n,k}\right)\left(v_S - v_{n,k}\right)\lambda_{n,k}S/L_{n,k} - v_{n,k}\left(1 - v_{n,k}\right)\lambda^h \\
&\tfrac{d}{dt}L^+_{n,k} = v_{n,k}\lambda^h L_{n,k} + \left(1 - p_f^+\right)\lambda_{n,k}S^+ + \left(h^+ + \left(1 - q_n\right)\gamma^+\right)I^+_{n,k} - \left(\mu^+ + \pi^+_{n,k} + \varepsilon^+\sum_{n,k}p^+_{n,k}\lambda_{n,k}\right)L^+_{n,k} \qquad \text{(S3)} \\
&\tfrac{d}{dt}I_{n,k} = p_{n,k}\lambda_{n,k}S + \pi_{n,k}L_{n,k} + \varepsilon p_{n,k}\lambda_{n,k}L - \left(\mu_T + h + \left(1 - q_n + q_n^{acq}\Big|_{n<n_{\max}}\right)\gamma + \left(n-k\right)\xi\right)I_{n,k} + \\
&\qquad + q_{n-1}^{acq}\gamma I_{n-1,k}\Big|_{n>k} + \left(n-k+1\right)\xi I_{n,k-1}\Big|_{k>0} \\
&\tfrac{d}{dt}I^+_{n,k} = p^+_{n,k}\lambda_{n,k}S^+ + \pi^+_{n,k}L^+_{n,k} + \varepsilon^+ p^+_{n,k}\lambda_{n,k}L^+ - \left(\mu_T^+ + h^+ + \left(1 - q_n + q_n^{acq}\Big|_{n<n_{\max}}\right)\gamma^+ + \left(n-k\right)\xi\right)I^+_{n,k} + \\
&\qquad + q_{n-1}^{acq}\gamma^+ I^+_{n-1,k}\Big|_{n>k} + \left(n-k+1\right)\xi I^+_{n,k-1}\Big|_{k>0} \\
&\lambda_{n,k} \equiv \beta^+ I^+_{n,k} + \beta I_{n,k} \\
&\lambda^h \equiv \beta^h\left(S^+ + L^+ + I^+\right) + \lambda^h_{boost}
\end{aligned}
$$

The parameters $\mu$, $\mu^+$, $\mu_T$, and $\mu_T^+$ are the natural, HIV-induced, TB-induced, and HIV/TB-induced death rates; $p_{n,k}$ and $p^+_{n,k}$ are the probabilities for fast progression to TB disease after infection with strain (n,k); $\pi_{n,k}$, and $\pi^+_{n,k}$ are the rates of endogenous reactivation to TB disease from latent infected with strain (n,k); $\varepsilon$ and $\varepsilon^+$ are the susceptibilities to reinfection with *M. tuberculosis*; $h$ and $h^+$ are the rates to self-cure from TB disease; $\xi$ is the rate of fitness compensation; $z$ is the initial fraction of those who are at risk of infection with HIV. The parameters $\gamma$ and $\gamma^+$ are the rates of detection/treatment initiation for individuals with active TB disease; $q_n$ is the probability of failing treatment or relapsing after treatment; $q_n^{acq}$ is the probability of amplifying resistance if treated. The vertical lines in some terms indicate the condition in which the term is included.

$\lambda_{n,k}$ is the infection force for each *M. tuberculosis* strain (n,k) and $\lambda^h$ is the infection force for HIV:

$$
\begin{aligned}
&\lambda_{n,k} = \beta^+ I^+_{n,k} + \beta I_{n,k} \\
&\lambda^h = \beta^h\left(S^+ + \sum_{n,k}\left(L^+_{n,k} + I^+_{n,k}\right)\right) + \delta\lambda^h
\end{aligned}
\quad , \qquad \text{(S4)}
$$

where $\beta$ and $\beta^+$ are the TB transmission coefficients, $\beta^h$ is the HIV transmission coefficient, and $\delta\lambda^h$ is a short-term perturbation of the force of infection, used to introduce HIV into a population.

The descriptions and assumed values of the parameters $\mu$, $\mu^+$, $\mu_T$, $\mu_T^+$, $\varepsilon$, $\varepsilon^+$, $h$, $h^+$, $\xi$, $z$, $\beta$, $\beta^+$, and $\beta^h$ are summarized in Table S1.

The parameters $p_{n,k}$, $p^+_{n,k}$, $\pi_{n,k}$, $\pi^+_{n,k}$, $\gamma$, $\gamma^+$, $q_n$, $q_n^{acq}$, and $\delta\lambda^h$ are more complex as they are either specific to each TB strain, or have intrinsic time-dependence, or both. We discuss each of them here.

The total number of ODE in (S3), $N_{eq}$, depends on the maximal number of resistances allowed for the model ($n_{\max}$) and is equal to:

$$N_{eq} = 3 + 5\frac{(n_{\max}+1)(n_{\max}+2)}{2} \ . \qquad \text{(S5)}$$

Thus, for $n_{\max}$ = 0/1/2/3/4 the ODE system (S3) contains 8/18/33/53/78 equations; for each figure in the main text the value of $n_{\max}$ is set to the maximal number of resistances among the strains shown on the figure.

**Risks of TB disease after infection.** In the model, both the probability of fast progression to TB and the rate of endogenous reactivation are functions of strain fitness $f_{nk}$ that depends on the costs of drug resistance conferring mutations ($\Delta f$) and the restoration effects of compensatory mutations ($\Delta f^c$). In the model we assume the costs and compensations have a multiplicative effect on capacity for bacterial propagation:

$$f_{nk} = \exp\left(-n\Delta f + k\Delta f^c\right). \qquad \text{(S6)}$$

Specifically for the values of $\Delta f = 0.07$ and $\Delta f^c = 0.06$ assumed in Table S1, the expression in the right part of (S6) reduces fitness by a factor of 1.073 with every resistance-conferring mutation and increases the fitness by a smaller factor of 1.062 with every compensatory mutation.

In order to cause disease, the *M. tuberculosis* strain must overwhelm a host's defensive ability, represented in the model by fitness thresholds $f_{thr}$ and $f^+_{thr}$. We assume that the overall risk of disease due to a strain is proportional to the excess fitness over this threshold; as such, in the model, we calculate the probability of fast progression and rate of reactivation from latency as being proportional to this difference:

$$\begin{aligned} &\frac{p_{nk}}{p} = \frac{\pi_{nk}}{\pi} = \frac{f_{nk} - f_{thr}}{1 - f_{thr}}; \qquad p_{nk},\, \pi_{nk} = 0 \ \ if \ \ f_{nk} < f_{thr} \\ &\frac{p^+_{nk}}{p^+} = \frac{\pi^+_{nk}}{\pi^+} = \frac{f_{nk} - f^+_{thr}}{1 - f^+_{thr}}; \qquad p^+_{nk},\, \pi^+_{nk} = 0 \ \ if \ \ f_{nk} < f^+_{thr} \end{aligned} \ , \qquad \text{(S7)}$$

where $p$, $p^+$, $\pi$, and $\pi^+$ are the corresponding parameters for DS strain: $f_{00} = 1$. The overall probability to develop TB disease after infection (determined by (S7)) is sensitive to both the fitness of the *M. tuberculosis* strain and HIV status of the host, as demonstrated by Figure S1.

The descriptions and assumed values of the parameters $p$, $p^+$, $\pi$, $\pi^+$, $\Delta f$, $\Delta f^c$, $f_{thr}$, and $f^+_{thr}$ are presented in Table S1.

**TB case detection and treatment.** The parameters $\gamma$ and $\gamma^+$ are the rates for the individuals with TB disease to be found and treated. Under the strong assumption of equal probability of finding active TB disease for HIV-positive and HIV-negative individuals, these rates are linked to the probability of case-detection ($0 < c_F < 1$) as follows:

$$\frac{\gamma}{\mu_T + h} = \frac{\gamma^+}{\mu^+_T + h^+} = \frac{c_F}{1 - c_F} \ . \qquad \text{(S8)}$$

The effects of varying this assumption of equal probability of TB case detection for those with and without HIV are shown Figure 7c of the main text.

The proportion of active TB cases detected ($c_F$) has significantly improved over the last two decades. We introduce it as a time-dependent parameter, which we estimated by log regression and fit to data from Swaziland [22] (shown on the figure S2a):

$$c_F(t) \approx \frac{1}{1 + Exp\left(0.548 - 0.009\left(t - 2000\right)\right)} \ . \qquad \text{(S9)}$$

In order to vary the case detection rate in the sensitivity analysis, we implemented a scaling parameter $\zeta^{detect}$ (described in Table S1) into (S8) as follows:

$$\frac{\gamma}{\mu_T + h} = \frac{\gamma^+}{\mu_T^+ + h^+} = \zeta^{detect} \frac{c_F}{1 - c_F} \quad . \tag{S10}$$

**Risk of TB treatment failure.** The parameter $q_n$ represents the probability of failing treatment for TB (or experiencing relapse after treatment). In the model, we assume that this probability of failure decreased over several decades as new TB drugs were introduced and better treatment programs were initiated (i.e. DOTS) and increases as a function of the number of drugs to which the infecting *M. tuberculosis* strain is resistant (*n*). We estimate $q_n$ as a function of the average treatment success probability $T_S$ as follows:

$$q_n = 1 - T_S \frac{1 - F_n}{1 - F_0} \quad , \tag{S11}$$

where $F_n$ is the probability of failure (or relapse) after standardized treatment regimen for a bacterial type with *n* resistances at the beginning of treatment. We estimate $F_n$ by a linear regression of the data [79] for the overall probability of treatment failure and relapse after treatment (shown on the figure S2b):

$$F_n \approx \zeta^{fail} \frac{6.9 + 12.7\, n}{100} \quad . \tag{S12}$$

Here $\zeta^{fail}$ is a scaling parameter used in the sensitivity analysis (described in Table S1).

We estimate the time-varying probability of treatment success $T_S$ by a double-log regression of the data from [22] (shown on the figure S2a):

$$T_S(t) \approx \frac{1 - F_0}{1 + \frac{1}{\zeta^{success}} Exp\left(0.614 - \frac{1.609}{1 + Exp\left((2005 - t)/2\right)}\right)} \quad . \tag{S13}$$

Here $\zeta^{success}$ is a scaling parameter for the sensitivity analysis (described in Table S1).

**Amplification of drug resistance during treatment for TB.** The parameter $q_n^{acq}$ represents the probability of acquiring resistance per treatment course. We assume that this parameter is proportional to the probability of either treatment failing or the individual relapsing after treatment:

$$\frac{q_n^{acq}}{q_n} \approx \frac{\eta}{1 + Exp\left((startyear_n - t)/2\right)} \quad . \tag{S14}$$

Here $\eta$ is the probability of acquiring resistance to an additional drug after the failure of treatment (described in Table 1S).

The time dependence in (S14) reflects an assumption that TB disease dominated by strains resistant to a particular anti-TB drug will not happen before the drug has been introduced. While this does not accurately model the actual dates on which the drugs became available and entered combined treatment regimens, for simplicity we assumed that one new drug entered the treatment regimen at the beginning of each of the following decades:

$$startyear = \{1960,\ 1970,\ 1980,\ 1990,...\} \quad . \tag{S15}$$

Due to relatively low case detection/treatment rates, as well as low prevalence of HIV, in the years prior to 1980, the subsequent model predictions do not depend strongly on this assumption of how and when the drugs were introduced.

**Initiation of HIV epidemics.** We simulate the initial emergence of HIV by applying a short-term perturbation to the force of infection of HIV $\lambda^h$ (see equation S6) in the following form:

$$\delta\lambda^h = \begin{cases} \delta\lambda^h_{peak} \left(\frac{t-1960}{20}\right)^2 Exp\left(2 - \frac{t-1960}{10}\right); & t > 1960 \\ 0; & t \le 1960 \end{cases} . \quad \text{(S16)}$$

The scaling parameter of the perturbation ($\delta\lambda^h_{peak}$) is used in the model to regulate the timing of HIV emergence. We adjusted this parameter in order to fit the time-dependencies of TB and HIV to the data from Swaziland [22]:

$$\delta\lambda^h_{peak} = 0.0000139/years . \quad \text{(S17)}$$

We have tested the model over the various forms of (S16) and found that if the timing of HIV epidemics peak is preserved, then all the time-trajectories, shown in main text, remain unchanged.

**Fitting the model to Swaziland data.** A least square method is used to fit the model to the data from Swaziland [22]. A reasonably good fit for the time-trends of TB incidence and HIV prevalence, shown in the main text (Figure 3a), is obtained by a variation of only three model parameters: the transmission coefficient of TB ($\beta$), regulating the reproductive number of TB infection; the transmission coefficient of HIV ($\beta^h$), regulating the reproductive number of HIV infection, and the parameter of initiation of HIV epidemics ($\delta\lambda^h_{peak}$), regulating the timing of the HIV peak.

Additionally, we modified the fitness cost of drug resistance ($\Delta f$) and the chance of drug resistance amplification after treatment failure ($\eta$) to allow the model to represent the current values of the frequency of MDRTB among new (7.7%) and retreatment (34%) cases of TB in Swaziland [22].

**Social mixing.** The main results presented in the text assume homogeneous mixing. In some settings individuals of like HIV status are more likely to be in contact with each other than would be expected by chance; this might reflect social preferences or concentration of individuals in nosocomial settings. We introduce the effect of inhomogeneous mixing into the equation system (S3) using the following simplifications for a structure of individual contacts providing the TB transmission:

1. The average number of respiratory contacts for a given individual does not depend on HIV status of individual.
2. The duration of average contact between the two individuals ($\Delta t^{contact}$) is short, compared to characteristic times of TB natural history; the loose ends from broken connections are being immediately reconnected on a random basis.
3. The HIV-assortative contacts are being broken with different regularity than disassortative ones ($\Delta t^{contact}_{same} \neq \Delta t^{contact}_{opposite}$). This allows to intensify the transmission between those of like HIV status without altering the total number of transmission events.

The mixing parameter ($\chi$) is introduced as a ratio of the durations of assortative and disassortative contacts:

$$\chi = \Delta t^{contact}_{same} / \Delta t^{contact}_{opposite} . \quad \text{(S18)}$$

If $\chi$>1, the individuals tend to attract the people with the same HIV status (assortative mixing), whereas if $\chi$<1 – the opposite is the case (disassortative mixing). In the presence of inhomogeneous mixing ($\chi \neq 1$), the exposure to TB infection by strain (n,k) is different for HIV-negative and HIV-positive individuals and cannot be described by a single infectious force $\lambda_{n\,k}$ (S4). Instead we have two different infectious forces ($\lambda^-_{n\,k}$ and $\lambda^+_{n\,k}$) for the individuals of different HIV status:

$$\begin{aligned}\lambda^{-}_{n\,k} &= m_{00}\beta I_{n\,k} + m_{01}\beta^{+} I^{+}_{n\,k} \\ \lambda^{+}_{n\,k} &= m_{10}\beta I_{n\,k} + m_{11}\beta^{+} I^{+}_{n\,k}\end{aligned} \quad . \tag{S19}$$

Here the mixing matrix ***m*** is:

$$m = \begin{pmatrix} \frac{2(1+\Omega)\chi^2}{1+\Omega\left(2\chi^2-1\right)+\sqrt{(1-\Omega)^2+4\Omega\chi^2}} & \frac{2(1+\Omega)}{1+\Omega+\sqrt{(1-\Omega)^2+4\Omega\chi^2}} \\ \frac{2(1+\Omega)}{1+\Omega+\sqrt{(1-\Omega)^2+4\Omega\chi^2}} & \frac{2(1+\Omega)\chi^2}{\Omega+2\chi^2-1+\sqrt{(1-\Omega)^2+4\Omega\chi^2}} \end{pmatrix}, \tag{S20}$$

where $\Omega$ is the ratio of HIV+ and HIV- prevalences:

$$\Omega = \frac{S^{+} + L^{+} + I^{+}}{S + L + I} \quad . \tag{S21}$$

The coefficients of matrix *m* represent how much the mixing increase (or decrease) the risk of transmission of TB between the two random individuals with given HIV status (0 – for HIV-negative; 1 – for HIV-positive).

In the limit of homogeneous mixing ($\chi \to 1$), the coefficients of matrix ***m*** approach unity and the expressions for the both forces of infection transform to the one in (S4):

$$\begin{aligned} m &= \begin{pmatrix} 1 & 1 \\ 1 & 1 \end{pmatrix} \\ \lambda^{-}_{n\,k} &= \lambda^{+}_{n\,k} = \beta I_{n\,k} + \beta^{+} I^{+}_{n\,k} \end{aligned} \quad . \tag{S22}$$

If a weak mixing is allowed ($|\chi - 1| << 1$), the equations (S19-S20) can be simplified as:

$$\begin{aligned} m &\approx \begin{pmatrix} 1 + \frac{\Omega^2}{(1+\Omega)^2}(\chi-1) & 1 - \frac{\Omega}{(1+\Omega)^2}(\chi-1) \\ 1 - \frac{\Omega}{(1+\Omega)^2}(\chi-1) & 1 + \frac{1}{(1+\Omega)^2}(\chi-1) \end{pmatrix} \\ \lambda^{-}_{n\,k} &\approx \lambda_{n\,k} - (\chi-1)\frac{\Omega}{(1+\Omega)^2}\left(\beta^{+} I^{+}_{n\,k} - \Omega\beta I_{n\,k}\right) \\ \lambda^{+}_{n\,k} &\approx \lambda_{n\,k} + (\chi-1)\frac{1}{(1+\Omega)^2}\left(\beta^{+} I^{+}_{n\,k} - \Omega\beta I_{n\,k}\right) \end{aligned} \quad . \tag{S23}$$

According to (S23), the reduction in infection force for individuals of one HIV-status is always compensated by increased infection force for the individuals of the other HIV-status. Assuming that the relative impact of HIV-positive individuals to the TB infectious force is usually higher (because of the known boost that HIV provides to TB prevalence):

$$\frac{\beta^{+} I^{+}_{n\,k}}{S^{+} + L^{+} + I^{+}} > \frac{\beta I_{n\,k}}{S + L + I} \quad , \tag{S24}$$

and therefore:

$$\beta^{+} I^{+}_{n\,k} - \Omega\beta I_{n\,k} > 0 \quad , \tag{S25}$$

the assortative mixing ($\chi > 1$) in (S23) reduces the exposure to TB for HIV-negative individuals ($\lambda^{-}_{n\,k} < \lambda_{n\,k}$) and increases it for HIV-positive ones ($\lambda^{+}_{n\,k} > \lambda_{n\,k}$).

In a limit of strong assortative mixing ($\chi \to \infty$), the individual has respiratory contacts only with hosts of the same HIV status:

$$
\begin{aligned}
m &= \begin{pmatrix} 1+\Omega & 0 \\ 0 & 1+\dfrac{1}{\Omega} \end{pmatrix} \\
\lambda^{-}_{n\,k} &= (1+\Omega)\beta I_{n\,k} \quad , \\
\lambda^{+}_{n\,k} &= \left(1+\frac{1}{\Omega}\right)\beta^{+} I^{+}_{n\,k}
\end{aligned}
\tag{S26}
$$

and the spread of *M. tuberculosis* occurs independently in HIV-positive and HIV-negative groups.

The full system of differential equations (S3) can be rewritten for the case of mixing as:

$$
\begin{aligned}
&\tfrac{d}{dt} S = \mu - \left(\mu + \sum_{n\,k} \lambda^{-}_{n\,k} + v_S \lambda^{h}\right) S \\
&\tfrac{d}{dt} v_S = (z - v_S)\,\mu / S - v_S (1 - v_S)\lambda^{h} \\
&\tfrac{d}{dt} S^{+} = v_S \lambda^{h} S - \left(\mu^{+} + \sum_{n\,k} \lambda^{+}_{n\,k}\right) S^{+} \\
&\tfrac{d}{dt} L_{n\,k} = (1 - p_{n\,k})\lambda^{-}_{n\,k} S + \left(h + (1 - q_n)\gamma\right) I_{n\,k} - \left(\mu + \pi_{n\,k} + \varepsilon \sum_{n\,k} p_{n\,k} \lambda^{-}_{n\,k}\right) L_{n\,k} \\
&\tfrac{d}{dt} v_{n\,k} = (1 - p_{n\,k})(v_S - v_{n\,k})\lambda^{-}_{n\,k} S / L_{n\,k} - v_{n\,k}(1 - v_{n\,k})\lambda^{h} \\
&\tfrac{d}{dt} L^{+}_{n\,k} = v_{n\,k}\lambda^{h} L + (1 - p^{+}_{f})\lambda^{+}_{n\,k} S^{+} + \left(h^{+} + (1 - q_n)\gamma^{+}\right) I^{+}_{n\,k} - \left(\mu^{+} + \pi^{+}_{n\,k} + \varepsilon^{+} \sum_{n\,k} p^{+}_{n\,k} \lambda^{+}_{n\,k}\right) L^{+}_{n\,k} \\
&\tfrac{d}{dt} I_{n\,k} = p_{n\,k}\lambda^{-}_{n\,k} S + \pi_{n\,k} L_{n\,k} + \varepsilon p_{n\,k}\lambda^{-}_{n\,k} L - \left(\mu_T + h + \left(1 - q_n + q^{acq}_{n}\Big|_{n<n_{\max}}\right)\gamma + (n-k)\xi\right) I_{n\,k} + \\
&\qquad + q^{acq}_{n-1}\gamma I_{n-1\,k}\Big|_{n>k} + (n-k+1)\xi I_{n\,k-1}\Big|_{k>0} \\
&\tfrac{d}{dt} I^{+}_{n\,k} = p^{+}_{n\,k}\lambda^{+}_{n\,k} S^{+} + \pi^{+}_{n\,k} L^{+}_{n\,k} + \varepsilon^{+} p^{+}_{n\,k}\lambda^{+}_{n\,k} L^{+} - \left(\mu^{+}_{T} + h^{+} + \left(1 - q_n + q^{acq}_{n}\Big|_{n<n_{\max}}\right)\gamma^{+} + (n-k)\xi\right) I^{+}_{n\,k} + \\
&\qquad + q^{acq}_{n-1}\gamma^{+} I^{+}_{n-1\,k}\Big|_{n>k} + (n-k+1)\xi I^{+}_{n\,k-1}\Big|_{k>0} \\
&\lambda^{h} = \beta^{h}\left(S^{+} + \sum_{n\,k}\left(L^{+}_{n\,k} + I^{+}_{n\,k}\right)\right) + \lambda^{h}_{boost}
\end{aligned}
\tag{S27}
$$

The solution of ODE system (S27) for $\chi = 2$ is shown on figure 7b in the main text.

**Initial conditions and model simulation.** We first allow the system to equilibrate in the absence of HIV; this yields an endemic incidence level of TB of approximately 200/100,000 persons per year. We then introduce TB treatment and HIV coinfection as described above. The code is written for Mathematica 8 [80].

**Sensitivity and uncertainty analysis.** Following [21], we used Latin Hypercube Sampling (LHS) to generate a total of 3000 parameter sets. Distributions and ranges for parameters sampled are listed in Table S1. Figure S3a demonstrates that the time-trajectory of individual level association (*PR*) between HIV and MDR-TB is robust against the variation of the basic model parameter set. This is illustrated by a tornado diagram on figure S3b, showing that the variation of even the most influential parameters within their uncertainty ranges cannot alter the average rate at which the association increases by more than 10% of its value.

Trends of Partial Rank Correlation Coefficients (PRCCs) depicted in Figure S4 demonstrate which parameters the absolute value of *PR* is most sensitive to over time. As it is partially shown by the figure

7a of the main text, this association is most sensitive to the parameters relating to fitness of strains and fitness thresholds of hosts ( $\Delta f^c$ , $f_{thr}$ , and $f^+_{thr}$ ). Nevertheless, as it is shown by figure S3, the absolute impact of even these parameters on the time-trajectory of association is small.

**Modeling of the alternative scenario of the failure of the measurements for TB control.** The predictions, generated within the base scenario of our model, for the future trends of TB incidence in total and MDR burden in particular, may appear too optimistic for some settings of Sub-Saharan Africa. Indeed, a persistent improvement of the measures for tuberculosis detection and treatment, while preserving the situation in other respects, cannot result in anything but a stable decline of TB rates over the time. Moreover, a decline of MDRTB burden specifically is predicted to be even more pronounced because of a) decreased acquisition (due to improvement of treatment success) and b) impaired transmission (as we have, in this model assumed MDRTB to be associated with fitness costs which may in reality not be true).

However, a stable decline in TB incidence rates (as was seen in much of Europe and North America) may not be replicated in Sub-Saharan Africa settings. This may be caused by either failure in improvement of anti-TB measures, or appearance of the other factors promoting the spread of TB, or both. In order to verify whether the conclusions we made about the individual level association between MDRTB and HIV remain applicable even in this case, we performed additional simulations (figure S5), which differ from the baseline simulations in two ways:

1. We assume that both the case-finding and treatment success probability do not improve and remain low (compare it with the expressions in S9 and S13):

$$\begin{aligned} c_F(t) &= 0.3 \\ T_S(t) &= 0.3\ (1 - F_0) \end{aligned} . \qquad \text{(S28)}$$

2. We assume that internal vulnerability of the population to TB infection is slowly increasing with the time, due to demographic growth or urbanization. In a simplest form, this can be introduced to the equation system S3 by modification of the first equation of the system:

$$\tfrac{d}{dt} S = \mu\, \alpha(t) - \left( \mu + \sum_{n\,k} \lambda_{n\,k} + v_S \lambda^h \right) S \ , \qquad \text{(S29)}$$

where $\alpha(t)$ represents an increased influx to the Susceptible class due to increase in birth rates or relocation of the people from country to cities, either of which may increase spread of TB. For simulation, shown on the figure, we assumed the dependence:

$$\alpha(t) = 1 + \frac{2Exp\left(\frac{t-2020}{20}\right)}{2 + Exp\left(\frac{t-2020}{20}\right)} \qquad \text{(S30)}$$

that provides a small increase starting in 1980-s, reaching approximately 1.2%/year currently, and reaching a threefold saturation in the future.

The two panels on the figure S5 reproduce the figures 3b and 4a from the main text, but generated with assumptions S28-S30. The population growth together with perpetuation of sub-optimal treatment results in an increase in the incidence of all the TB strains (figure 5a). Nevertheless, while the relative frequencies of MDRTB are monotonically increasing (figure 5b, black lines), the individual level association between MDRTB and HIV is very similar to the base-scenario trend presented in the main text of the paper (thick vs thin gray lines on the panel).

**Combination of the effects may explain high values of *PR*:** As we have shown by sensitivity analysis above (Figures 6 and S4), only a limited range of the MDRTB prevalence ratio values ($0.5 < PR < 1.5$) can be explained by the differences in natural histories of TB infection between HIV-positive and HIV-negative individuals, such are the differences in progression rates, immune response strength, and duration of the disease. A new study from Swaziland [20] finds the value of the prevalence ratio to be $PR \approx 2$ in 2010, both for acquired and transmitted MDRTB strains. Figure S6 shows that our model can reproduce the value of $PR=2$ in 2010 (upper panel) by simultaneous present of multiple mechanisms. Here, as an example, we a) set a higher level of "fitness threshold" for HIV-negative individuals that reduces the vulnerability of immunocompetent individuals to low-fit MDRTB strains and b) set a higher level of case-finding for HIV-positive individuals with TB disease, both effects combine to produce an increased PR over our baseline model which only considers these mechanism in isolation.

***Supplementary References***


18. C. Dye, B.G. Williams, M.A. Espinal, M.C. Raviglione, Erasing the World's Slow Stain: Strategies to Beat Multidrug-Resistant Tuberculosis. *Science* **295**, 2042-46 (2002).
20. E. Sanchez-Padilla, T. Dlamini, A. Ascorra, S. Rusch-Gerdes, Z.D. Tefera, P. Calain, R. de la Tour, F. Jochims, E. Richter, M. Bonnet, High Prevalence of Multidrug-Resistant Tuberculosis, Swaziland, 2009–2010. *Emerging Infectious Diseases* **18**, 29-37 (2012).
21. S.M. Blower and H. Dowlatabadi, Sensitivity and Uncertainty Analysis of Complex Models of Disease Transmission: An HIV Model, as an Example. *International Statistical Review* **62**, 229-43 (1994).
22. *Tuberculosis country profiles* (WHO's global TB database, World Health Organization, Geneva, Switzerland, 2011, available at http://www.who.int/tb/country/data/profiles/en/index.html).
24. T. Cohen, M. Murray, Modeling epidemics of multidrug-resistant M-tuberculosis of heterogeneous fitness. *Nature Medicine* **10**, 1117-21 (2004).
35. S. Basu, J.R. Andrews, E.M. Poolman, N.R. Gandhi, N.S. Shah, A. Moll, P. Moodley, A.P. Galvani, G.H. Friedland, Prevention of nosocomial transmission of extensively drug-resistant tuberculosis in rural South African district hospitals: an epidemiological modelling study. *Lancet* **370**, 1500-07 (2007).
42. S. Borell, S. Gagneux, Strain diversity, epistasis and the evolution of drug resistance in Mycobacterium tuberculosis. *Clinical Microbiology and Infection* **17** 815-820 (2011).
58. C. Dye and B.G. Williams, Slow Elimination of Multidrug-Resistant Tuberculosis. *Science Translational Medicine* **1**, 3ra8 (2009).
62. E. Vynnycky and P.E.M. Fine, The Natural History of Tuberculosis: The Implications of Age-Dependent Risks of Disease and the Role of Reinfection. *Epidemiology and Infection* **119**, 183-201 (1997).
63. I. Sutherland, E. Svandova, S. Radhakrishna, The Development of Clinical Tuberculosis Following Infection with Tubercle-Bacilli. *Tubercle* **63**, 255-68 (1982).
71. *Estimation and Projection Package 2009* (UNAIDS manual for generalized epidemics, Joint United Nations Programme on HIV/AIDS, 2009, available at http://www.unaids.org/en/dataanalysis/tools/epp2009/).
74. S. Gagneux, C.D. Long, P.M. Small, T. Van, G.K. Schoolnik, B.J.M. Bohannan, The Competitive Cost of Antibiotic Resistance in Mycobacterium tuberculosis. *Science* **312**, 1944-6 (2006).

79. W. Lew, M. Pai, O. Oxlade, D. Martin, D. Menzies, Initial Drug Resistance and Tuberculosis Treatment Outcomes: Systematic Review and Meta-analysis. *Annals of Internal Medicine* **149**, 123-34 (2008).
80. Mathematica 8.0.1.0 for Mac OSX x86, Wolfram Research Inc.
81. S. Allen, J. Batungwanayo, K. Kerlikowske, A.R. Lifson, W. Wolf, R. Granich, H. Taelman, P. Vandeperre, A. Serufilira, J. Bogaerts, G. Slutkin, P.C. Hopewell, Two-year incidence of tuberculosis in cohorts of HIV infected and uninfected urban Rwandan women. *American Review of Respiratory Diseases* **146**, 1439-44 (1992).
82. D. Mulder, A. Nunn, A. Kamali, J. Nakiyingi, H.U. Wagner, J.F. Kengeyakayondo, Two-year HIV-1 associated mortality in a Ugandan rural population. *Lancet* **343**, 1021-3 (1994).
83. A. Pablos-Mendez, T.R. Sterling, T.R. Frieden, The relationship between delayed or incomplete treatment and all-cause mortality in patients with tuberculosis. *The Journal of the American Medical Association* **276**, 1223-8 (1996).
84. H.E. Hilleboe, Post-sanatorium tuberculosis survival rates in Minnesota. *Public Health Reports* **56**, 895-907 (1941).
85. G. Berg, The prognosis of open pulmonary tuberculosis. A clinical statistical analysis. *Acta Tuberculosea Scandinavica suppl* **4**, 1-207 (1939).
86. G. Drolet, Present trend of case fatality rates in tuberculosis. *American Review of Tuberculosis* **37**, 125-51 (1938).
87. V. Springett, Ten-year results during the introduction of chemotherapy for tuberculosis. *Tubercle* **52**, 73-87 (1971).
88. C.R. Lowe. Recent trends in survival of patients with respiratory tuberculosis. *British Journal of Preventive and Social Medicine* **8**, 91-8 (1954).
89. National Tuberculosis Institute, Bangalore, Tuberculosis in a rural population in South India: a five year study. *Bulletin of the World Health Organization* **51**, 473 (1974).
90. B. Thompson, Survival rates in pulmonary tuberculosis. *British Medical Journal* **2**, 721 (1943).
91. P.M. Small, G.F. Schecter, P.C. Goodman, M.A. Sande, R.E. Chaisson, P.C. Hopewell, Treatment of Tuberculosis In Patients with Advanced Human-Immunodeficiency-Virus Infection. *New England Journal of Medicine* **324**, 289 (1991).
92. F. Palmieri, A.M. Pellicelli, E. Girardi, A.P. de Felici, P. de Mori, N. Petrosillo, G. Ippolito, Negative predictors of survival in HIV-infected patients with culture-confirmed pulmonary tuberculosis. *Infection* **27**, 331-4 (1999).
93. P. Nunn, R. Brindle, L. Carpenter, Cohort study of human immunodeficiency virus infection in patients with tuberculosis in Nairobi, Kenya: analysis of early (6 month) mortality. *American Review of Respiratory Diseases* **146**, 849-54 (1992).
94. J.H. Perriens, M.E. st Louis, Y.B. Mukadi, C. Brown, J. Prignot, F. Pouthier, F. Portaels, J.C. Willame, J.K. Mandala, M. Kaboto, R.W. Ryder, G. Roscigno, P. Piot, Pulmonary tuberculosis in HIV-infected patients in Zaire: a controlled trial of treatment for either 6 or 12 months. *New England Journal of Medicine* **332**, 779-84 (1995).
95. J.A. Rutledge, J.B. Crouch, The ultimate results in 1694 cases of tuberculosis treated at the Modern Woodmen Sanitorium of America. *American Review of Tuberculosis* **2**, 755-6 (1919).
96. W.H. Tattersall, The survival of sputum positive consumptives. A study of 1192 cases in a county borough between 1914 and 1940. *Tubercle* **28**, 85-96 (1947).
97. T. Madsen, J. Holm, K.A. Jensen, Studies on the epidemiology of tuberculosis in Denmark. *Acta Tuberculosea Scandinavica suppl* **6**, 1-176 (1942).
98. S. Bergqvist, T. Ernberg, Zur Frage der tuberkulosen Primarinfektion bei jungen Erwachsenen. *Acta Medica Scandinavica* **115**, 57-82 (1943).
99. C. Daley, P. Small, G. Schecter, G.K. Schoolnik, R.A. Mcadam, W.R. Jacobs, P.C. Hopewell, An outbreak of tuberculosis with accelerated progression among persons infected with the human immunodeficiency virus. *New England Journal of Medicine* **326**, 231-35 (1992).

100. G. di Perri, M. Danzi, G. Dechecchi, S. Pizzighella, M. Solbiati, D. Bassetti, M. Cruciani, R. Luzzati, M. Malena, R. Mazzi, E. Concia, Nosocomial epidemic of active tuberculosis among HIV - infected patients. *Lancet* **2**, 1502-04 (1989).
101. P. Nunn, M. Mungai, J. Nyamwaya, C. Gicheha, R.J. Brindle, D.T. Dunn, W. Githui, J.O. Were, K.P.W.J. Mcadam, The effect of human immunodeficiency virus type-1 on the infectiousness of tuberculosis. *Tubercle and Lung Disease* **75**, 25-32 (1994).
102. G. Barnett, S. Grzybowski, K.M. Styblo, Present risk of developing active tuberculosis in Saskatchewen according to previous tuberculin and X-ray status. *Bulletin of the International Union Against Tuberculosis* **45**, 51-74 (1971).
103. G.W. Comstock, V.T. Livesay, S.F. Woolpert, The Prognosis of a Positive Tuberculin Reaction in Childhood and Adolescence. *American Journal of Epidemiology* **99**, 131-8 (1974).
104. K. Styblo, Epidemiology of Tuberculosis. *The Hague, Royal Netherlands Tuberculosis Association KNCV* (1991).
105. C.B. Holmes, R. Wood, M. Badri, S. Zilber, B.X. Wang, G. Maartens, H. Zheng, Z.G. Lu, K.A. Freedberg, E. Losina, CD4 decline and incidence of opportunistic infections in Cape Town, South Africa: Implications for prophylaxis and treatment. *Journal of Acquired Immune Deficiency Syndromes* **42**, 464-9 (2006).
106. C.F. Gilks, P. Godfrey-Faussett, B.I.F. Batchelor, J.C. Ojoo, S.J. Ojoo, R.J. Brindle, J. Paul, J. Kimari, M.C. Bruce, J. Bwayo, F.A. Plummer, D.A. Warrell, Recent transmission of tuberculosis in a cohort of HIV-1-infected female sex workers in Nairobi, Kenya. *AIDS* **11**, 911-8 (1997).
107. J.R. Glynn, Resurgence of tuberculosis and the impact of HIV infection. *British Medical Bulletin* **54**, 579-93 (1998).
108. P.A. Selwyn, D. Hartel, V.A. Lewis, E.E. Schoenbaum, S.H. Vermund, R.S. Klein, A.T. Walker, G.H. Friedland, A Prospective-Study of the Risk of Tuberculosis Among Intravenous Drug-Users with Human Immunodeficiency Virus-Infection. *New England Journal of Medicine* **320**, 545-50 (1989).
109. C. Dye, B.G. Williams, Eliminating human tuberculosis in the twenty-first century. *Journal of the Royal Society Interface* **5**, 653-662 (2008).
110. G.M. Cauthen, S.W. Dooley, I.M. Onorato, W.W. Ihle, J.M. Burr, W.J. Bigler, J. Witte, K.G. Castro, Transmission of Mycobacterium Tuberculosis from Tuberculosis Patients with HIV infection of AIDS. *American Journal of Epidemiology* **44**, 69-77 (1996).
111. R. Colebunders, R. Ryder, N. Nzilambi, K. Dikilu, J.C. Willame, M. Kaboto, N. Bagala, J. Jeugmans, K. Muepu, H.L. Francis, J.M. Mann, T.C. Quinn, P. Piot, HIV infection in patients with tuberculosis in Kinshasa, Zaire. *American Review of Respiratory Disease* **139**, 1082-85 (1989).
112. K.M. de Cock, E. Gnaore, G. Adjorlolo, M.M. Braun, M.F. Lafontaine, G. Yesso, G. Bretton, I.M. Coulibaly, G.M. Gershydamet, R. Bretton, W.L. Heyward, Risk of tuberculosis in patients with HIV-I and HIV-II infections in Abidjan, Ivory Coast. *British Medical Journal* **301**, 496-99 (1991).
113. A. Elliott, R. Hayes, B. Halwiindi, N. Luo, G. Tembo, J.O.M. Pobee, P.P. Nunn, K.P.W.J. Mcadam, The impact of HIV infectiousness of pulmonary tuberculosis: a community study in Zambia. *AIDS* **7**, 981-7 (1993).
114. W. Githui, P. Nunn, E. Juma, F. Karimi, R. Brindle, R. Kamunyi, S. Gathua, C. Gicheha, J. Morris, M. Omwega, Cohort study of HIV-positive and HIV-negative tuberculosis, Nairobi, Kenya: comparison of bacteriological results. *Tubercle and Lung Disease* **73**, 203 (1992).
115. P. Sonnenberg, J. Murray, S. Shearer, J.R. Glynn, B. Kambashi, P. Godfrey-Faussett, Tuberculosis treatment failure and drug resistance-same strain or reinfection?. *Transactions of the Royal Society of Tropical Medicine and Hygiene* **94**, 603-7 (2000).

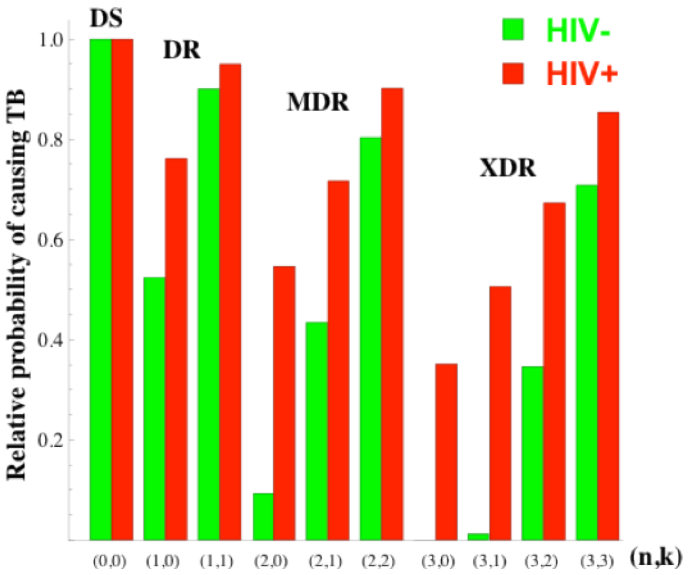


**Figure S1. Fitness costs for the strains**
Fitness-dependent reduction in the probability of fast progression and the rates of endogenous reactivation (equation S7). The coefficient for the DS strain is set to 1 as the referent category. The x-axis shows the strains arranged according to the number of drug resistant mutations (n) and compensatory events (k). Green bars represent relative probabilities for strains to cause TB in HIV-seronegative hosts and the red bars represent the same probabilities for HIV-seropositive hosts.

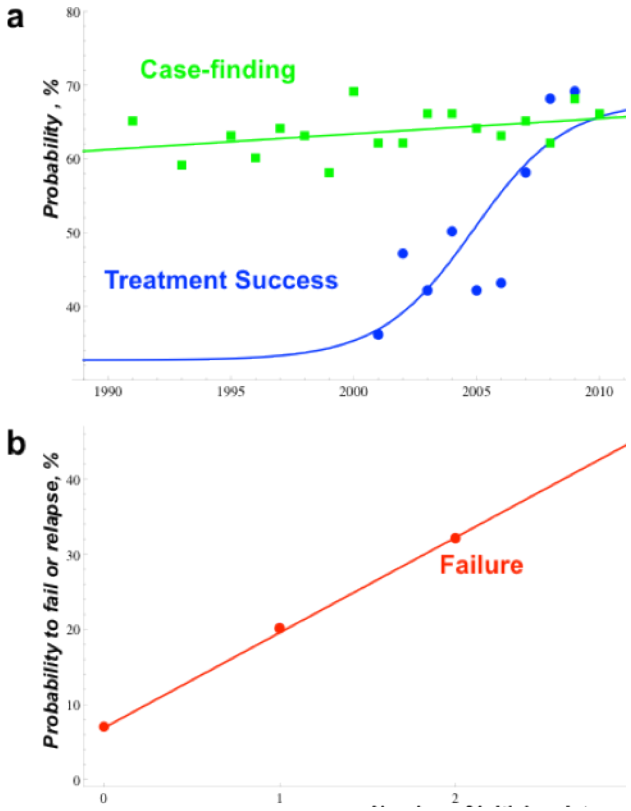


**Figure S2. Assumed patterns for case-finding, treatment success and failure chance**
**a)** Time-varying treatment success (blue, see also equation S13) and case-finding (green, equation S9) adopted for the model. The dots represent the data from [22].

**b)** Assumed relationship between baseline number of drugs to which the infecting *M. tb.* strain is resistant and probability of failure or immediate relapse from standardized 4-drug treatment regimen. The horizontal axis shows the initial number of drugs the bacteria is resistant to at the beginning of treatment (see equation S12). The dots represent the data from [79] for a total probability of failure and relapse for a patient, harboring DS, DR, or MDR TB strains.

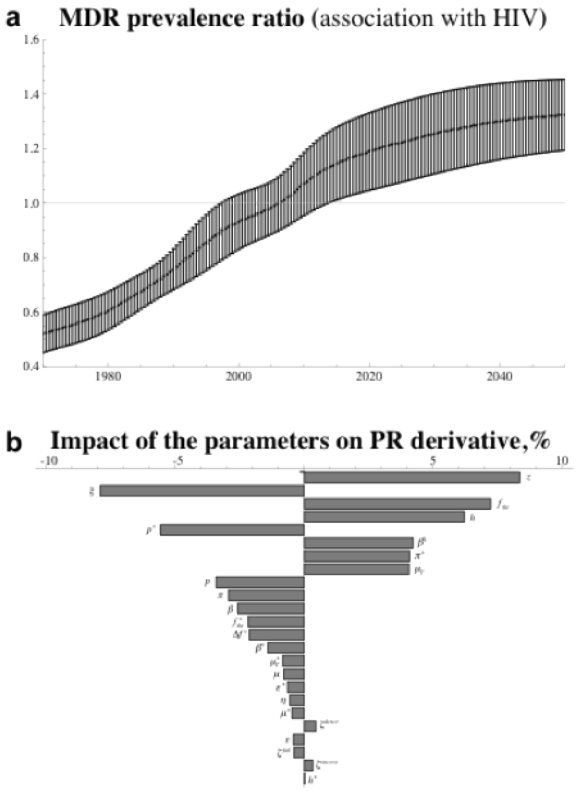


**Figure S3. Uncertainty analysis**
Uncertainty analysis for the individual-level association (*PR*) between MDRTB and HIV MDRTB: **a)** The multivariate uncertainties in association time-trend (this panel is also shown as figure 6a in the main text). The mean value is shown by the dotted line; the standard deviation is shown by bars. **b)** A tornado diagram of univariate effects of the model parameter uncertainties on average time-derivative of MDRTB prevalence ratio for the years 1980-2040.

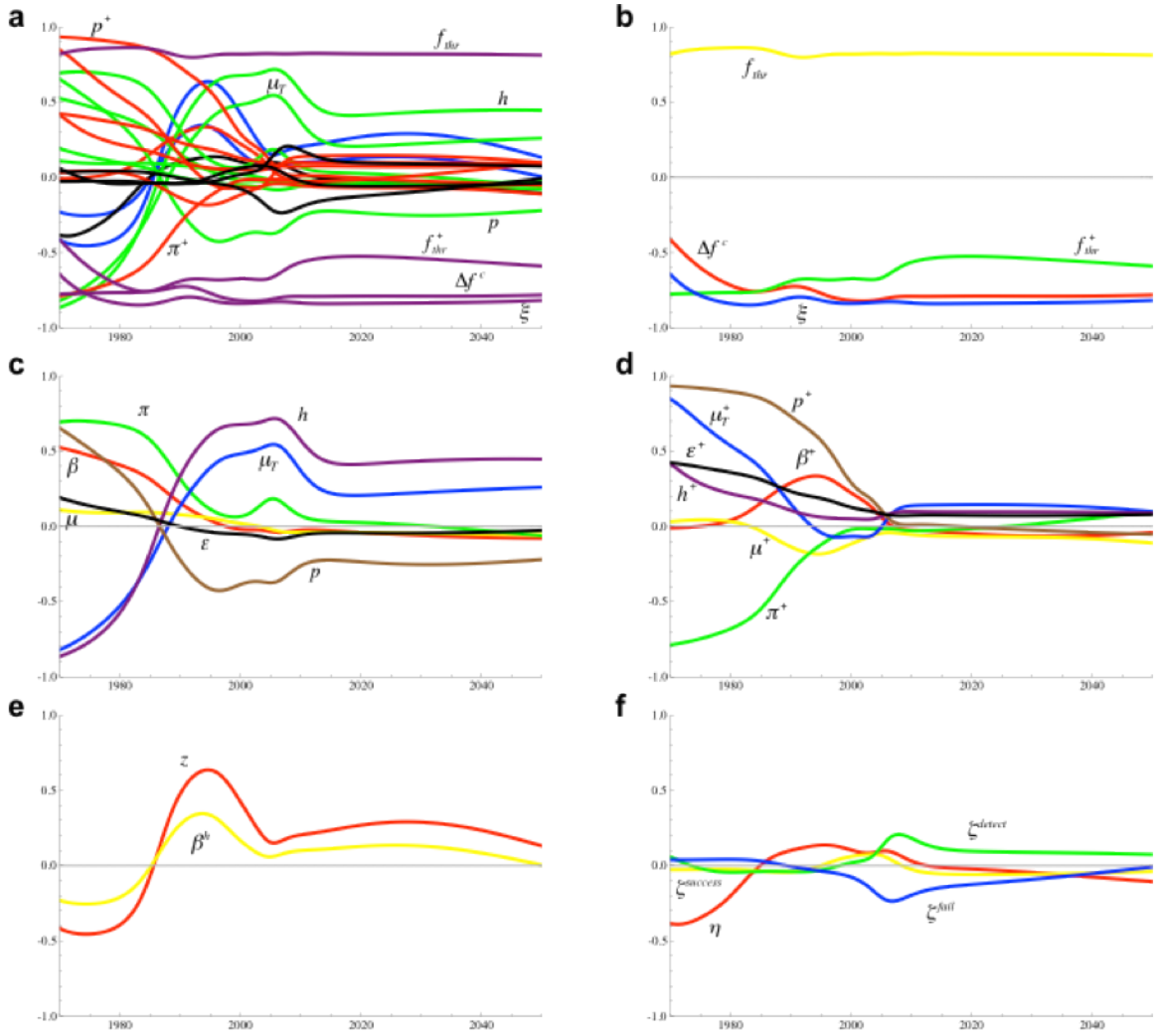


**Figure S4. Partial rank correlation coefficients**
Multivariable sensitivity analysis. The partial rank correlation coefficients between the ratio of the prevalences (*PR*) of drug-resistance between HIV-seropositive and HIV-seronegative hosts with TB disease and the model parameters. Latin hypercube sampling is used for 24 model parameters subjected to variation within assumed ranges (Table S1). For better visualization, we split the parameters into 5 groups and represent them by 6 panels:
**a)** All parameters. Colors represent related parameters which are disaggregated in other panels.

**b)** Parameters related to fitness (purple on the panel a): $\Delta f^c$ (red); $f_{thr}$ (yellow); $f_{thr}^+$ (green); and $\xi$ (blue).

**c)** Parameters related to natural history of TB in HIV-seronegative hosts (green on the panel a): $\beta$ (red); $\mu$ (yellow); $\pi$ (green); $\mu_T$ (blue); $p$ (brown); $h$ (purple); and $\varepsilon$ (black).

**d)** Parameters related to natural history of TB in HIV-seropositive hosts (red on the panel a): $\beta^+$ (red); $\mu^+$ (yellow); $\pi^+$ (green); $\mu_T^+$ (blue); $p^+$ (brown); $h^+$ (purple); and $\varepsilon^+$ (black).

**e)** Parameters related to HIV (blue on the panel a): $z$ (red); and $\beta^h$ (yellow).

**f)** Parameters related to treatment (black on the panel a): $\eta$ (red); $\zeta^{success}$ (yellow); $\zeta^{detect}$ (green); and $\zeta^{fail}$ (blue).

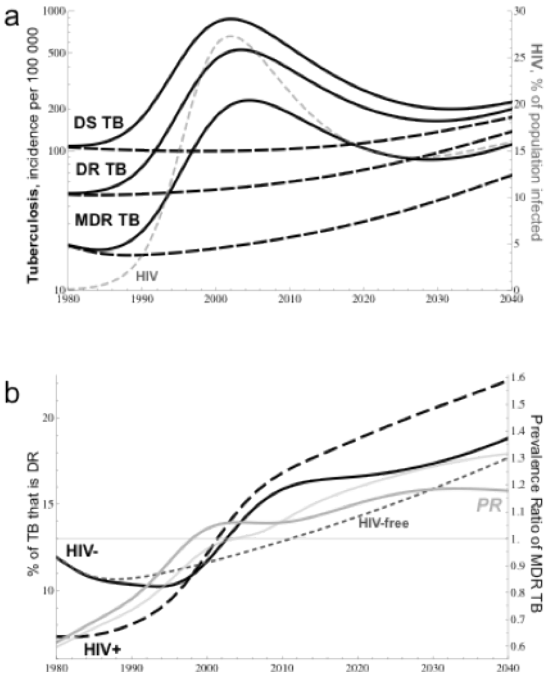


**Figure S5. Simulation of pessimistic scenario for MDRTB control**

Simulation results (compare with figures 3b and 4a from the main text) for a growing population without improvement in TB treatment over time (see equations S28-S30).

**a)** Trends of the incidence of drug sensitive, drug resistant, and multi-drug resistant in populations with epidemic HIV (solid lines) and without HIV (thick dashed lines). The trend in the prevalence of HIV (which drives the rise in TB incidence shown in the solid traces) is shown by the thin dashed line

**b)** Projected trends in the percentage of TB incidence that is with MDR strains. The trends for HIV+ and HIV- individuals within populations with epidemic HIV are represented by black dashed lines and black solid lines, respectively. The trend for individuals in populations unaffected by HIV is shown with a thin gray dashed line. The gray solid line shows the prevalence ratio of drug-resistance between HIV-seropositive and HIV-seronegative hosts (PR right axis) in the population with epidemic HIV. A thin gray line represent the prevalence ratio for base-scenario model (figure 4a) shown for a reference.

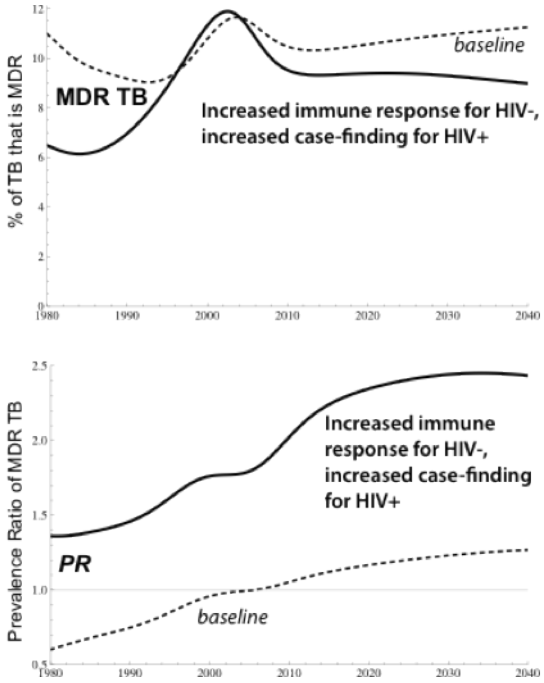


**Figure S6. Cumulative effect of the mechanisms promoting HIV-MDRTB association**

Effect of simultaneous variation of the fitness thresholds for those without HIV infection and the relative probability of case detection. The upper panel indicate the trend in the proportion of TB that is MDR and lower panel indicate the trend in the individual-level relative risk of MDR among HIV-seropositive and HIV-seronegative hosts with TB. Solid line: $f_{thr} = 0.9$ and the probability of case detection is set to be twice as high for a HIV-coinfected TB patient than a TB patient without HIV; thin dashed line shows baseline model simulation for a reference.

| Param. | Description | Value | Sensitivity Analysis [1]Range | [2]Effect on PR | | References and Notes |
|---|---|---|---|---|---|---|
| $\mu$ | Non-TB death rates of adult hosts | 0.023/year | (0.022-0.024) | + | − | 0.023 [35] |
| $\mu^+$ | | 0.098/year | (0.088-0.108) | + | − | 0.044 [81]; 0.116 [82] |
| $\mu_t$ | TB-specific death rates hosts | 0.26/year | (0.19-0.33) | −−− | ++ | 0.35 [83]; 0.3 [84]; 0.3 [85]; 0.3 [86]; 0.43 [87]; 0.35 [88]; 0.2 [89]; 0.51 [90]. The first-year estimates are shown. In all the studies the mortality rate drops ~40% after the first year. |
| $\mu_t^+$ | | 0.82/year | (0.64-1.00) | ++ | + | 0.47 [81]; 0.88 [83]; 0.75 [91]; 0.79 [92]; 3.7 $\mu_t$ [93]; 0.37 [94] |
| $h$ | Rate of self-cure of TB individuals | 0.2 | (0.1-0.3) | −−− | ++ | 0.2 [89]; From the fraction of survivals after 5+ years: 0.97 $\mu_t$ [85]; 0.58 $\mu_t$ [87]; 0.75 $\mu_t$ [89]; 0.42 $\mu_t$ [90]; 0.77 $\mu_t$ [95]; 0.43 $\mu_t$ [96] |
| $h^+$ | | 0 | (0.0-0.5) $h$ | ++ | + | The value is set to 0 in calculations, but is varied in sensitivity analysis |
| $p$ | Probability of fast progression to TB | 0.11 | (0.08-0.14) | ++ | −− | 0.11 [62]; 0.055 [63]; 0.13 [81] (our estimation); 0.13 [97]; 0.11 [98] |
| $p^+$ | | 0.46 | (0.25-0.67) | +++ | − | 0.37 [99]; 0.44 [100]; 4.1 $p$ [101] |
| $\varepsilon$ | Susceptibility to TB reinfection | 0.35 | (0.30-0.40) | + | + | 0.59 [62]; 0.377 [63] |
| $\varepsilon^+$ | | 0.75 | (0.65-0.85) | ++ | + | 0.75 [35] (assumed) |
| $\pi$ | Rate of endogenous reactivation from latency | 0.0011/year | (0.8-1.4) $10^{-3}$ | +++ | − | 3 $10^{-4}$ [62]; 1.4 $10^{-4}$ [63]; 3 $10^{-4}$ [102]; 9 $10^{-4}$ [103]; 1.5 $10^{-4}$ [104] |
| $\pi^+$ | | 0.04/year | (0.03-0.05) | −−− | + | 0.08 [105]; 0.04 [106]; 0.05 [107]; 0.08 [108] |
| $\beta$ | TB transmission rate | 4.9/year /person | (4.4-5.4) | ++ | − | The parameter is used to fit TB incidence trend from Swaziland [22]. Consistent with: 7.8 [109] (averaged between all the forms of TB) |
| $\beta^+$ | | 0.7 $\beta$ | (0.5-0.9) $\beta$ | + | − | 1.5 $\beta$ [101]; 0.59 $\beta$ [110]; 0.53 $\beta$ [111]; 0.59 $\beta$ [112]; 0.43 $\beta$ [113]; 1.0 $\beta$ [114] |
| $\beta^h$ | HIV transmission coefficient | 0.93/year /person | (0.84-1.02) | −− | + | The parameter is used to fit HIV prevalence trend from Swaziland [22]. |
| $\eta$ | Probability of DR acquisition per treatment failure | 0.87 | (0.78-0.96) | −− | − | The parameter is used to fit current MDR frequency among retreatment cases in Swaziland [22]; 0.1÷0.4 [58]; 0.3 [79]; 0.4 [115] |
| $\xi$ | Rate of fitness compensation | 0.1/year | (0.033-0.300) | −−− | −−− | Assumed. Log-uniform distribution has been assigned for sensitivity analysis |
| $\Delta f$ | Relative fitness cost per drug-resistant mutation | 0.07 | - | NA | NA | The value is used to fit current MDR frequency among new cases in Swaziland [22]; 0.1÷0.4 [74]; excluded from the sensitivity analysis due to inter-dependence with $f_{thr}$ and $f_{thr}^+$ (Eq. S6-S7) |
| $\Delta f^c$ | Relative fitness gain per compensation event | 0.06 | (0.8-1.0) $\Delta f$ | −−− | −−− | The value may be close to $\Delta f$, as some clinical strains show low reduction in fitness and ability to compensate initial fitness costs [42,74] |
| $f_{thr}$ | Minimum fitness threshold for TB disease | 0.8 | (0.75-0.85) | +++ | +++ | The value provides plausible estimation for reduction in transmission of MDR strain with low, average and high fitness (Eq. S7): 0.35; 0.62; and 0.90. It is consistent with estimation: 0.3 [18]; and assumptions of [24]: 0.3-0.7. |
| $f_{thr}^+$ | | 0.6 | (0.6-0.9) $f_{thr}$ | −−− | −−− | The threshold is assumed to be lower in immunocompromised hosts |
| $z$ | Fraction of population influx that is susceptible to HIV infection | 0.5 | (0.4-0.6) | −− | ++ | [71], calibrated to generate realistic HIV epidemic |
| $\zeta^{detect}$ | TB case detection tuning parameter | 1 | (0.9-1.1) | − | + | |
| $\zeta^{success}$ | TB treatment success tuning parameter | 1 | (0.9-1.1) | − | − | The parameters are used to test the model sensitivity to estimates of case detection, treatment success and failure rate (see figure S2 and equations S10, S12-13). |
| $\zeta^{fail}$ | TB treatment failure probability tuning parameter | 1 | (0.9-1.1) | + | − | |

[1] A uniform distribution over the shown range has been assigned to each parameter, unless stated otherwise.
[2] The effect of the parameter variation on MDRTB-HIV association. The sign of correlation is shown by either "+" or "-"; the strength of correlation is shown by number of signs: 1-non significant effect ($|PRCC|<0.2$); 2-moderate ($0.5>|PRCC|\geq 0.2$); 3-significant ($|PRCC|\geq 0.5$)). The two columns represent the time-periods of early (before 1985) and late (after 2010) HIV epidemics.